Doppler-aided positioning in GNSS receivers - A performance analysis

François Vincent [a,*], Jordi Vilà-Valls [a], Olivier Besson [a], Daniel Medina [b], Eric Chaumette [a]

[a] University of Toulouse/ISAE-SUPAERO, 10 Avenue Edouard Belin, Toulouse, France
[b] Institute of Communications and Navigation, German Aerospace Center (DLR), Neustrelitz, Germany

Keywords:
GNSS
Positioning
Cramér-Rao bound
Fisher information matrix
Multilateration
High-sensitivity
Harsh propagation conditions

A B S T R A C T

The main objective of Global Navigation Satellite Systems (GNSS) is to precisely locate a receiver based on the reception of radio-frequency waveforms broadcasted by a set of satellites. Given delayed and Doppler shifted replicas of the known transmitted signals, the most widespread approach consists in a two-step algorithm. First, the delays and Doppler shifts from each satellite are estimated independently, and subsequently the user position and velocity are computed as the solution to a Weighted Least Squares (WLS) problem. This second step conventionally uses only delay measurements to determine the user position, although Doppler is also informative. The goal of this paper is to provide simple and meaningful expressions of the positioning precision. These expressions are analysed with respect to the standard WLS algorithms, exploiting the Doppler information or not. We can then evaluate the performance improvement brought by a joint frequency and delay positioning procedure. Numerical simulations assess that using Doppler information is indeed effective when considering long observation times, and particularly useful in challenging scenarios such as urban canyons (constrained satellite visibility) or near indoor situations (weak signal conditions which need long integration times), thus providing new insights for the design of robust and high-sensitivity receivers.

1. Introduction

The main objective of Global Navigation Satellite Systems (GNSS) is to provide precise position, velocity and time (so-called PVT solution) to any user on Earth, thanks to the transmission of electromagnetic (EM) signals broadcasted from a constellation of satellites [1]. The PVT estimates are obtained by exploiting the modifications that these EM waves undergo during their travel from the different satellites in view to the receiver. More precisely for any kind of band-limited transmitted signal

$$e(t) = c(t)e^{2i\pi f_0 t}, \tag{1}$$

where $c(t)$ represents the baseband signal and f_0 the carrier frequency, the received signal $r(t)$ can be written, up to a scaling factor and under the narrowband assumption [2,3], as

$$r(t) = \alpha e(t-\tau) + n(t) = \alpha c(t-\tau)e^{2i\pi f_0(t-\tau)} + n(t), \tag{2}$$

where α is a complex channel gain and $n(t)$ is a thermal noise term, which in general may also include any other unmodelled effect such as multipath. For short time periods, given the transmitter to receiver range d_0 and range rate $\dot{d}_0$, the delay τ can be can be approximated by a first order model,

$$\tau = \frac{d_0}{c} + \frac{\dot{d}_0}{c}t = \tau_0 + \epsilon t, \tag{3}$$

so that

$$r(t) \simeq \left[c(t-\tau_0)e^{-2i\pi f_0\tau_0}e^{-2i\pi f_0\epsilon t}\right]e^{2i\pi f_0 t} \tag{4}$$

where the delay drift ϵ can be neglected inside the baseband signal $c(t)$.

From (4) it is easy to identify that the transmitted signal undergo 3 main modifications, namely, a pure delay of the baseband signal, τ_0, a constant phase shift, $-2i\pi f_0\tau_0$, and a frequency shift, $-f_0\epsilon$. The two first effects are linked to the distance d_0, whereas the latter, so-called Doppler effect, is linked to the range rate $\dot{d}_0$. Both range and range rate are in turn related to the receiver position and velocity to be inferred. The standard way to exploit this information to estimate the receiver PVT from the reception of EM waves from multiple beacons (i.e., satellites) is to follow a two-step approach. In the first step, the range and range rate for each transmitter to receiver link are estimated, thus computing a set of estimates to all visible satellites in parallel. This can be done thanks to the GNSS signal design where the different transmitted $c(t)$ must have a very low cross-correlation among different satellites. The goal of the second step is to fuse these individual transmitter to receiver estimates solving a multilateration problem, which is usually

* Corresponding author.
E-mail address: francois.vincent@isae.fr (F. Vincent).

https://doi.org/10.1016/j.sigpro.2020.107713

done through a Weighted Least Square (WLS) procedure [4]. This popular two-step approach has been shown to be asymptotically equivalent [5] to the one-step Maximum Likelihood (ML) solution, so-called Direct Positioning Estimator (DPE) [6,7], which directly estimates the receiver position and velocity from the received signal. Although the two-step procedure is usually suboptimal in real-life non-nominal conditions, the high computational complexity of the DPE prevents its use in mass-market applications (i.e., DPE implies a ML search on a high-dimensional space). That is the reason why the conventional two-step solution is still the gold standard.[1]

As it has been pointed out right above, one can exploit three different measurements from the received EM signals to estimate the receiver position:

- The simplest and widespread positioning approach, being the state-of-the-art solution, only exploits the delay carried by the baseband signal $c(t-\tau_0)$, conducting to the estimation of so-called *pseudoranges* (i.e., *pseudo* because transmitters and receiver are not synchronized and the signal experiments delays during its pass through the atmosphere). From a set of pseudoranges a multilateration step is performed to compute the receiver position, that is, the intersection of a set of spheres, roughly speaking. Notice that even if not exploited for the final position computation, the Doppler shifts must be also estimated to obtain a correct delay estimate.
- A more precise solution, consists in exploiting the additional phase information in (4), namely, $-2i\pi f_0\tau_0$. Indeed, this measurement is linked to the wavelength which is much smaller than the baseband signal resolution (i.e., for a legacy Global Positioning System (GPS) L1 C/A signal, the wavelength is approximately 19 cm while the baseband signal resolution is 300 m). Unfortunately, exploiting this phase information implies solving a much more complicated problem, mainly because the carrier phase measurement is ambiguous (i.e., unknown number of cycles inside the baseband signal resolution), then being such ambiguity resolution the bottleneck ([4], Chap 21, Chap 23). To this end two different schemes can be advocated. The first approach to resolve phase ambiguities is to turn to the class of so-called differential techniques, where the relative position to a geo-referenced GNSS station is obtained. Real-Time Kinematics (RTK) ([4], Chap 26) is an example of such a technique. Nevertheless, this kind of solution requires the use of a reference station with a communication link between the two receivers, and is only valid for short ranges from the base-station to ensure that the two receivers observe the same propagation errors. Another approach is the family of Precise Point Positioning (PPP) techniques ([4], Chap 25), which allow to get rid of the reference station but to reach decimetric precision in turn need (i) precise carrier phase measurements, which is not the case in harsh propagation conditions, (ii) high accuracy satellite orbits, clock and propagation (ionospheric and tropospheric) error corrections, and/or (iii) multi-frequency/multi-system architectures to compensate ionospheric effects. These kind of techniques received much attention in the literature (see [8] and references therein) and are still under research to reach the maturity needed for their broad real-time applicability. The price to be paid is the need to access a network broadcasting real-time precise corrections (i.e., International GNSS Service (IGS) products), and a long convergence time of tens of minutes. As stated in [8], these drawbacks limit the use of PPP for many practical real-time applications. Phase-based positioning approaches are out of the scope of this contribution.
- Finally, referring to (4), the last measurement that can be exploited to infer information on the receiver position is the Doppler effect. Indeed, since this term is linked to the range rate, and because the position and velocity vectors of the transmitter are known a-priori, it brings information on both the receiver velocity and its position through the Line-of-Sight (LOS) direction. It is important to notice that this last information on the position is an angular information and not a ranging one, thus supplementing the two other measurements. Although this information has historically been at the core of the former GPS, namely Transit, it is seldom used in modern GPS receivers. The reasons of this lack of interest in Doppler positioning is certainly due to its poor precision compared to ranging measurements, at least for short observation times. Nevertheless, its use is very simple and known to be more robust to harsh propagation environments such as urban canyons affected by dense multipath or in indoor conditions. One of the rare usage of this information in GPS receivers is an improved coarse positioning acquisition technique where Dopplers are exploited independently from the two other ranging measurements to speed up the initialization of the tracking process [9].

In this contribution we focus on the solutions exploiting both delay and Doppler measurements with the aim to provide a fundamental analysis and determine if it is worth considering, and under which conditions, Doppler information in GNSS positioning algorithms. To this end, we provide a simple and striking formulation of the covariance matrix on the position estimation based on both delay and Doppler measurements. In this formulation, we do not take into account the carrier phase information mentioned right above, mainly because this leads to very specific solutions which do not apply for standard standalone receivers. Nevertheless, the Cramér-Rao Bound (CRB) for a mixture of real and integer-valued parameters, and its use for carrier phase-based positioning techniques performance characterization, has been derived in [10].

When dealing with precision, a popular way to proceed is to determine the Fisher Information Matrix (FIM) or its inverse, the CRB, which gives a lower bound for the covariance matrix of the estimates. In the case of GNSS receivers, the FIM associated to the one-step ML solution (i.e., DPE) has been calculated in [11], but no insights on the performance associated to the delay/Doppler two-step approach were provided. Even if DPE has been shown to be asymptotically efficient, it suffers from a huge computational burden which prevents its use in real-time applications. On the other hand, the two-step approach is suboptimal because it relaxes the links existing among all delays and Dopplers and simply considers them as independent measurements. However, it has been recently shown to be asymptotically efficient when using an appropriated weighting [5]. Such optimal weights are obtained by resorting to the EXtended Invariance Principle (EXIP) [12], which states that using a re-parametrization of the problem can lead to a simpler solution while preserving the asymptotic performances. More precisely, the intermediate estimates obtained from a simpler first step can be refined to asymptotically achieve the performance of the initial model using an appropriate WLS minimization. Obviously, this optimal solution must exploit not only pseudoranges to each satellite in view (i.e., delays) but also Doppler measurements.

Although it is widely used in all GNSS receivers, the performance analysis of this two-step procedure through the determination of the corresponding receiver position covariance matrix (i.e., CRB) has not been properly handled in the literature. Indeed, [11] shows the performance difference between DPE and the two-step procedure, but the latter only considers delay measurements,

[1] Notice that DPE implies a 8-dimensional search using the baseband signal samples (i.e., typically at 4, 8 or 12 Msamples/s), and the two-step approach solution is given by a 2-dimensional search per satellite (baseband) plus the PVT solution at a rate which is at most 1kHz. The 2-dimensional delay/Doppler grid search in standard receivers, typically known as acquisition process, is the most time and power consuming stage of the receiver, therefore, a 8-dimensional grid search may become prohibitive in small platforms.

then missing all the information brought by Dopplers. Moreover, to the best of the author's knowledge, there is no complete (delay/Doppler) closed-form expression of the covariance matrix for the position estimates of the WLS two-step procedure. Of course, the concept of Geometric Dilution Of Precision (GDOP) has been introduced for a long time [1], but it only describes the second step of the processing and does not take into account the information brought by Dopplers. Several papers deal with the CRB in the context of radiolocation. For instance, in the reverse case of source localization thanks to synchronized sensors, the CRB has been calculated [13–17], but several differences prevent using these results in the GNSS case, namely the fact that the signal is unknown and considered as random in the case of passive localization. Other authors have calculated the CRB in the case of GNSS Reflectometry (GNSS-R) altimeters [18], but once again, many intrinsic differences about the processing prevent from adapting these results to the case of GNSS positioning.

In this contribution we derive the covariance matrix of the position estimation for any WLS procedure based on both delays and Dopplers. This result is valid for any kind of weighting, and especially for the optimal WLS scheme [5] conducting to the best precision. We obtain a simple and meaningful formulation of the precision one can obtain using a GNSS receiver, that clearly exhibits the improvement provided by the use of Dopplers when considering long integration times or in constrained satellite visibility. Of course, this formulation can also be exploited in the more standard way, where only the delays are taken into account. These results provide new insights to be exploited in harsh propagation conditions and especially meaningful for high-sensitivity GNSS receivers [19] (i.e., indoor GNSS), which are expected to be at the core of precise time synchronization for next generation 5G small cells. Notice that we do not consider specific multipath or indoor propagation conditions, but rather show analytically and through simulations that when using long integration times (i.e., as in HS-GNSS) or under constrained satellite geometries (i.e., being the case in urban conditions) the performance can be improved if properly using Dopplers.

The paper is organized as follows. First, the problem at hand and the two-step WLS procedure to estimate the user position are described in Section 2. Then, the covariance matrix of these estimates is derived in Section 3, and some insights for the standard weighting procedures are provided in Section 4. Section 5 allows to analyse in which configuration it is worth using Doppler measurements in addition to delay measurements, through numerical simulations. Concluding remarks are provided in Section 6.

2. Problem statement

2.1. Signal model

We assume that K scaled, delayed and Doppler-shifted front waves, transmitted by the set of satellites in view impinge on a GNSS receiver antenna. Under the narrowband assumption, the complex baseband model can be written as follows,

$$y(t) = \sum_{k=1}^{K} \alpha_k c_k(t-\tau_k) e^{-2i\pi f_0 b_k t} + n(t), \tag{5}$$

where the phase term in (4) is absorbed by the complex amplitudes α_k. This can be rewritten in a more compact form as,

$$\mathbf{y} = \mathbf{A}\boldsymbol{\alpha} + \mathbf{n}, \tag{6}$$

where

- $\mathbf{y} = [y(0) \dots y((N-1)T_s)]^T$, T_s being the sampling period and N the number of coherent available samples,
- $\mathbf{A} = [\mathbf{a}_1 \dots \mathbf{a}_K]$ is the manifold corresponding to all in-view satellite signals, with $\mathbf{a}_k = \mathbf{c}_k \odot \mathbf{e}_k$, where $\mathbf{c}_k = [c_k(-\tau_k) \cdots c_k((N-1)T_s - \tau_k)]^T$ is the sampled transmitted code for satellite k affected by the corresponding delay τ_k, and $\mathbf{e}_k = [1 \cdots e^{-2i\pi f_0 b_k (N-1)T_s}]^T$ its frequency signature due to the $f_k = -f_0 b_k$ Doppler shift, $\odot$ being the element-wise product,
- $\boldsymbol{\alpha} = [\alpha_1 \dots \alpha_K]^T$ the corresponding complex amplitudes,
- $\mathbf{n} = [n(0) \dots n((N-1)T_s)]^T$ the complex noise, assumed to be circularly white and Gaussian, with noise power σ^2.

The observed delay, τ_k, and delay drift, b_k, depend on the actual relative distance and velocity from satellite k to the receiver, as well as secondary propagation effects (ionospheric and tropospheric additional delays, ...) and receiver or transmitter defaults (clock bias and drift). They can be expressed as follows,

$$\tau_k \simeq \frac{||\mathbf{p}_k - \mathbf{p}||}{c} + \tau_0 + \delta\tau_k, \tag{7}$$

$$b_k \simeq \frac{(\mathbf{v}_k - \mathbf{v})^T.\mathbf{u}_k}{c} + b_0 + \delta b_k,$$

where

- $\mathbf{p}$, $\mathbf{v}$, $\mathbf{p}_k$ and $\mathbf{v}_k \in \mathbb{R}^3$ are, respectively, the position and velocity vectors of both receiver and k-th satellite,
- $\mathbf{u}_k = \frac{\mathbf{p}_k - \mathbf{p}}{||\mathbf{p}_k - \mathbf{p}||}$ is the unitary steering vector toward the k-th satellite,
- τ_0 and b_0 are the receiver clock delay and delay drift with respect to (w.r.t) the GNSS time reference,
- $\delta\tau_k$ and δb_k include all secondary biases (satellites clock defaults, propagation, ...) and are supposed to be known from the navigation message,
- c the celerity of EM waves.

The unknowns of the positioning problem can be gathered in vector $\boldsymbol{\zeta} = [\boldsymbol{\alpha}_r^T \boldsymbol{\theta}^T]^T$ where $\boldsymbol{\alpha}_r = [\mathrm{Re}\{\alpha_1\}\,\mathrm{Im}\{\alpha_1\} \cdots \mathrm{Re}\{\alpha_K\}\,\mathrm{Im}\{\alpha_K\}]^T$ is the vector of the signal amplitudes and $\boldsymbol{\theta} = [\mathbf{p}^T\, c\tau_0\, \mathbf{v}^T\, cb_0]^T$ is the 8-dimensional vector corresponding to the user position, velocity, clock delay and drift.

Notice that we can make explicit in (6) the dependence on $\boldsymbol{\theta}$, $\mathbf{y} = \mathbf{A}(\boldsymbol{\theta})\boldsymbol{\alpha} + \mathbf{n}$. If we assume the complex amplitudes $\boldsymbol{\alpha}$ as deterministic and unknown, it is straightforward to show that the DPE ML-based solution of the problem is given by maximizing the nonlinear following criterion [6],

$$\hat{\boldsymbol{\theta}}_{\mathrm{ML}} = \arg\max_{\boldsymbol{\theta}} \left[\mathbf{y}^H \mathbf{P}_{\mathbf{A}}(\boldsymbol{\theta})\mathbf{y}\right] \tag{8}$$

where $(\,\cdot\,)^H$ stands for the Hermitian transpose operation and the projection matrix onto the signal subspace, spanned by the K received signals, is $\mathbf{P}_{\mathbf{A}} = \mathbf{A}(\mathbf{A}^H\mathbf{A})^{-1}\mathbf{A}^H$. We can observe that $\mathbf{A}^H\mathbf{A} \simeq N\mathbf{I}$, as the GNSS pseudo-random codes broadcasted by the satellites are almost orthogonal and the Doppler shift modulations are relatively slow compared to the signal variations. This near orthogonality of the columns of $\mathbf{A}$ is the assumption that allows a separate processing for each satellite signal in all standard GNSS receiver. Therefore, we can simply write that

$$\hat{\boldsymbol{\theta}}_{\mathrm{ML}} \simeq \arg\max_{\boldsymbol{\theta}} \left[\left|\left|\mathbf{A}(\boldsymbol{\theta})^H\mathbf{y}\right|\right|^2\right] = \arg\max_{\boldsymbol{\theta}} \left[\sum_{k=0}^{K-1} |\mathbf{a}_k(\boldsymbol{\theta})^H\mathbf{y}|^2\right], \tag{9}$$

which is a nonlinear 8-dimensional optimization problem. Then, because of the near orthogonality condition, the original ML position estimation can be decoupled into K individual (reparametrized) ML delay/Doppler estimation problems, which are in turn fused to obtain the ML position solution [5].

2.2. Standard and optimal two-step solution

Given that the direct solution of (8) is difficult to implement in practice, as already stated, the classical way to estimate the

receiver position and velocity consists in a two-step procedure: i) first, the delays and Doppler shifts for each satellite signal are estimated, and then ii) a WLS procedure allows to estimate the receiver position and velocity. The first step of this algorithm corresponds to a ML procedure and is also performed in two stages. Indeed, as the electronic noise is assumed to be Gaussian and white, the ML is shown to be a 2D correlation maximization for each couple of unknowns τ_k and b_k. Conventionally, this maximization is first performed using a loose grid (acquisition stage) and then a local and tight smaller grid is used to track the maximum (tracking loops) in order to reduce the computational complexity. The output of the tracking stage is fed into the data demodulation block which allows to compute the so-called pseudoranges. Notice that time-delays (i.e., pseudoranges), Dopplers (i.e., pseudorange rates) and carrier phase observables are the main outputs of the synchronization stage of any receiver, typically obtained via delay/frequency/phase locked loop architectures. Therefore, delay and Doppler measurements are readily available in almost any commercial receiver. The second step of the procedure tends to estimate $\boldsymbol{\theta}$ from the nonlinear problem in (7). As the receiver usually gets an approximate initial solution (from the Bancroft algorithm [20], for instance), the standard way to solve this problem is to linearize (7) near an initial guess, $\boldsymbol{\theta}_0 = [\mathbf{p}_0^T\, c\tau_{00}\, \mathbf{v}_0^T\, cb_{00}]^T$,

$$\boldsymbol{\eta}_k \Delta= \begin{bmatrix} \tau_k - \frac{||\mathbf{p}_k - \mathbf{p}_0||}{c} - \delta\tau_k \\ b_k - \frac{(\mathbf{v}_k - \mathbf{v}_0)^T . \mathbf{u}_{k0}}{c} - \delta b_k \end{bmatrix} = \frac{1}{c}\mathbf{H}_k(\boldsymbol{\theta} - \boldsymbol{\theta}_0), \tag{10}$$

with

$$\mathbf{H}_k = \begin{bmatrix} -\mathbf{u}_{k0}^T & 1 & \mathbf{0}^T & 0 \\ -\boldsymbol{\nu}_{k0}^T & 0 & -\mathbf{u}_{k0}^T & 1 \end{bmatrix}, \tag{11}$$

where $\mathbf{u}_{k0} = \frac{\mathbf{p}_k - \mathbf{p}_0}{||\mathbf{p}_k - \mathbf{p}_0||}$ is the direction vector toward the k-th satellite from the supposed position $\mathbf{p}_0$ and $\boldsymbol{\nu}_{k0} = \frac{\mathbf{P}_{k0}^{\perp}\mathbf{v}_k}{||\mathbf{p}_k - \mathbf{p}_0||}$, with $\mathbf{P}_{k0}^{\perp}$ the projection matrix on the subspace orthogonal to $\mathbf{u}_{k0}$, corresponds to the angular velocity vector. Observing (11), it is noteworthy that the Doppler (or delay drift) depends on the velocity, but also on the position through this angular velocity vector. Hence, Dopplers bring a direct piece of information on the user position.

It is important to mention that standard GNSS receivers that use Dopplers to estimate the velocity, usually assume that the angular velocity vectors in the linerized matrix (11) are null, i.e., $\boldsymbol{\nu}_{k0} = \mathbf{0}$, and then do not exploit the totality of the Doppler information [21, Chap 7].

Using the linearized observation model, the ad-hoc procedure is a WLS closed-form solution,

$$\begin{aligned} \hat{\boldsymbol{\theta}} - \boldsymbol{\theta}_0 &= \arg\min_{\boldsymbol{\theta}} \big[c\boldsymbol{\eta} - \mathbf{H}(\boldsymbol{\theta} - \boldsymbol{\theta}_0)\big]^T \mathbf{W} \big[c\boldsymbol{\eta} - \mathbf{H}(\boldsymbol{\theta} - \boldsymbol{\theta}_0)\big] \\ &= c(\mathbf{H}^T\mathbf{W}\mathbf{H})^{-1}\mathbf{H}^T\mathbf{W}\boldsymbol{\eta} \end{aligned} \tag{12}$$

where $\boldsymbol{\eta} = \big[\boldsymbol{\eta}_1^T \ldots \boldsymbol{\eta}_K^T\big]^T$, $\mathbf{H} = \big[\mathbf{H}_1^T \ldots \mathbf{H}_K^T\big]^T$ and $\mathbf{W}$ is the diagonal weighting matrix, depending on the chosen WLS scheme. As stated before, the standard way to proceed, is to consider only the delay measurements in this WLS step, that simply consists in removing the corresponding lines in matrix $\mathbf{H}$ and vector $\boldsymbol{\eta}$. Two weights are conventionally used: (i) $\mathbf{W} = \mathbf{I}$, leading to a standard LS, or (ii) a weight related to the inverse of the measurement noise covariance, which is typically approximated as a function of the estimated signal-to-noise ratio (SNR) and/or the different satellites' elevation. In short, this is related to the received signal power and then, up to a scale factor, $\mathbf{W} = \mathrm{diag}(\boldsymbol{\alpha} \odot \boldsymbol{\alpha}^*)$ [4].

The optimal way to proceed would be to consider also the information contained in the Doppler. Considering Dopplers or not, the weighting matrix can be written as

$$\mathbf{W} = \begin{bmatrix} \mathbf{W}_\tau & \mathbf{O} \\ \mathbf{O} & \mathbf{W}_b \end{bmatrix}. \tag{13}$$

where $\mathbf{W}_\tau \Delta= \mathrm{diag}(\mathbf{w}^\tau)$ are the delays weighting and $\mathbf{W}_b \Delta= \mathrm{diag}\big(\mathbf{w}^b\big)$ the delay drifts weighting, leaved identically null if not considered in the WLS minimization. In [5], the optimal weighting is shown to be

$$\mathbf{W}_\tau = \beta\mathbf{P}_\alpha \text{ and } \mathbf{W}_b = \delta\mathbf{P}_\alpha \tag{14}$$

with

$$\beta = \frac{2\pi^2 N B^2}{3\sigma^2}, \tag{15}$$

$$\delta = \frac{2\pi^2 N(N-1)(N+1) f_0^2 T_s^2}{3\sigma^2}, \tag{16}$$

and

$$\mathbf{P}_\alpha = \mathrm{diag}(\boldsymbol{\alpha} \odot \boldsymbol{\alpha}^*),\ \mathbf{P}_\alpha(k,k) = |\alpha_k|^2, \tag{17}$$

B being the signal bandwidth.

3. Closed-form position covariance matrix (CRB) expression

The precision performance of this two-step procedure is contained in the covariance matrix of the estimate $\hat{\boldsymbol{\theta}}$ in (12). Assuming that the first step procedure reaches its asymptotic performance, this covariance matrix is obtained as [11]

$$\mathrm{cov}(\hat{\boldsymbol{\theta}}) = c^2(\mathbf{H}^T\mathbf{W}\mathbf{H})^{-1}\mathbf{H}^T\mathbf{W}\mathbf{F}_\eta^{-1}\mathbf{W}^T\mathbf{H}(\mathbf{H}^T\mathbf{W}\mathbf{H})^{-1}, \tag{18}$$

where $\mathbf{F}_{\boldsymbol{\eta}}$ is the right-lower block of the complete FIM $\mathbf{F}_{\boldsymbol{\gamma}}$ on the intermediate parameters $\boldsymbol{\gamma} = [\boldsymbol{\alpha}_r^T\, \boldsymbol{\eta}^T]^T$, whose (k, ℓ) element is given by

$$\mathbf{F}_{\boldsymbol{\gamma}}^{k,\ell} = \frac{2}{\sigma^2}\mathrm{Re}\left\{\frac{\partial(\mathbf{A}\boldsymbol{\alpha})^H}{\partial\boldsymbol{\gamma}_k}\frac{\partial(\mathbf{A}\boldsymbol{\alpha})}{\partial\boldsymbol{\gamma}_\ell}\right\}, \tag{19}$$

In order to obtain a closed-form expression of the covariance matrix (18), we have first to compute the FIM on the intermediate parameters given in (19).

3.1. FIM on the intermediate parameters

As shown in Appendix A, the intermediate parameters of the FIM can be written in the following block form,

$$\mathbf{F}_\gamma = \begin{bmatrix} \mathbf{A} & \mathbf{B} \\ \mathbf{B}^T & \mathbf{D} \end{bmatrix}, \tag{20}$$

with $\mathbf{A} = \frac{2N}{\sigma^2}\mathbf{I}_{2K}$,

$$\mathbf{B} = \frac{4\pi f_0 T_s \sum_{n=0}^{N-1} n}{\sigma^2}\mathrm{diag}\left(\begin{bmatrix} 0 & \mathrm{Im}\{\alpha_k\} \\ 0 & \mathrm{Re}\{\alpha_k\} \end{bmatrix}_{k=1:K}\right),$$

$$\mathbf{D} = \frac{8\pi^2}{\sigma^2}\mathrm{diag}\left(\begin{bmatrix} \frac{NB^2|\alpha_k|^2}{12} & 0 \\ 0 & f_0^2 T_s^2 |\alpha_k|^2 \sum_{n=0}^{N-1} n^2 \end{bmatrix}_{k=1:K}\right).$$

Using the block matrix inversion formula, it is readily seen that

$$\begin{aligned} \mathbf{F}_{\boldsymbol{\eta}}^{-1} &= \big[\mathbf{D} - \mathbf{B}^T\mathbf{A}^{-1}\mathbf{B}\big]^{-1} \\ &= \mathrm{diag}\left(\frac{\sigma^2}{8\pi^2|\alpha_k|^2}\begin{bmatrix} \frac{12}{NB^2} & 0 \\ 0 & (f_0^2 T_s^2 \mathrm{Var}\{n\})^{-1} \end{bmatrix}_{k=1:K}\right), \end{aligned} \tag{21}$$

with $\mathrm{Var}\{n\} = \frac{N(N-1)(N+1)}{12}$.

It can be noticed that thanks to the diagonal structure of $\mathbf{F}_{\boldsymbol{\eta}}^{-1}$, the CRB on the delays is simply $\mathbf{F}_\tau^{-1} = \frac{1}{\beta}\mathbf{P}_\alpha^{-1}$, and the CRB on the delay drifts is $\mathbf{F}_b^{-1} = \frac{1}{\delta}\mathbf{P}_\alpha^{-1}$, with $\mathbf{P}_\alpha$ defined in from Eq. (17). It

is noteworthy that the optimal weights introduced at the end of Section 2.2, $\mathbf{W}_\tau$ and $\mathbf{W}_b$, correspond to this FIM. Although this is only an intermediate result, it is interesting, as it gives precisely the asymptotic precision one can obtain on the delay and Doppler measurements in case of GNSS signals.

3.2. Covariance matrix (CRB) on the position estimation

The covariance matrix on the 8-D vector $\boldsymbol{\theta}$ can be computed from (18) and (21). Because we are interested in the receiver position we focus on the first 4 parameters of $\boldsymbol{\theta}$, $\mathbf{pos} = [\mathbf{p}^T \ (c\tau_0)]^T$, corresponding to the position. For that purpose we conduct a block matrix inversion of $\mathbf{H}^T\mathbf{W}\mathbf{H}$, which can be written

$$\mathbf{H}^T\mathbf{W}\mathbf{H} = \begin{bmatrix} (\mathbf{U}\mathbf{W}_\tau\mathbf{U}^T + \mathbf{V}\mathbf{W}_b\mathbf{V}^T) & \mathbf{V}\mathbf{W}_b\mathbf{U}^T \\ \mathbf{U}\mathbf{W}_b\mathbf{V}^T & \mathbf{U}\mathbf{W}_b\mathbf{U}^T \end{bmatrix}, \tag{22}$$

with $\mathbf{U} = \left[[-\mathbf{u}_{10}^T \quad 1]^T \dots [-\mathbf{u}_{K0}^T \quad 1]^T\right]$ and $\mathbf{V} = \left[[-\boldsymbol{v}_{10}^T \quad 0]^T \dots [-\boldsymbol{v}_{K0}^T \quad 0]^T\right]$. Hence, we have

$$(\mathbf{H}^T\mathbf{W}\mathbf{H})^{-1} = \begin{bmatrix} \boldsymbol{\Omega}^{-1} & \mathbf{B} \\ \mathbf{B}^T & - \end{bmatrix},$$

where

$$\boldsymbol{\Omega} = \mathbf{U}\mathbf{W}_\tau\mathbf{U}^T + \mathbf{V}\mathbf{W}_b^{1/2}\mathbf{P}_\perp\mathbf{W}_b^{1/2}\mathbf{V}^T,$$
$$\mathbf{B} = -\boldsymbol{\Omega}^{-1}\mathbf{V}\mathbf{W}_b\mathbf{U}^T(\mathbf{U}\mathbf{W}_b\mathbf{U}^T)^{-1},$$

with

$$\mathbf{P}_\perp = \mathbf{I} - \mathbf{W}_b^{1/2}\mathbf{U}^T(\mathbf{U}\mathbf{W}_b\mathbf{U}^T)^{-1}\mathbf{U}\mathbf{W}_b^{1/2}.$$

Then, using this block decomposition in (18), we can obtain the following covariance matrix for the position parameters only,

$$\begin{aligned}\mathrm{cov}(\mathbf{pos}) = c^2\boldsymbol{\Omega}^{-1}[&(\mathbf{U}\mathbf{W}_\tau^{1/2}\mathcal{F}_\tau^{-1}\mathbf{W}_\tau^{1/2}\mathbf{U}^T) \\ &+ (\mathbf{V}\mathbf{W}_b^{1/2}\mathbf{P}_\perp\mathcal{F}_b^{-1}\mathbf{P}_\perp\mathbf{W}_b^{1/2}\mathbf{V}^T)]\boldsymbol{\Omega}^{-1},\end{aligned} \tag{23}$$

where $\mathcal{F}_\tau^{-1} = \mathbf{W}_\tau^{1/2}\mathbf{F}_\tau^{-1}\mathbf{W}_\tau^{1/2}$ and $\mathcal{F}_b^{-1} = \mathbf{W}_b^{1/2}\mathbf{F}_b^{-1}\mathbf{W}_b^{1/2}$ are the normalized FIM on the delay and Dopplers. It has to be noticed that we simply have $\mathcal{F}_\tau^{-1} = \mathcal{F}_b^{-1} = \mathbf{I}$ when one chooses the optimal weights (14) for $\mathbf{W}_\tau$ and $\mathbf{W}_b$.

The result in (23) gives the position precision (i.e., CRB) associated to any GNSS WLS multilateration procedure whether Dopplers are used ($\mathbf{W}_b \neq \mathbf{0}$) or not ($\mathbf{W}_b = \mathbf{0}$). Obviously this performance depends on the number of satellites and their positions through the direction vectors $\mathbf{U}$, but also on their velocity through the angular velocity vectors $\mathbf{V}$. In the case of an optimal weighting (14), this last expression simplifies as we have $\mathcal{F}_\tau^{-1} = \mathcal{F}_b^{-1} = \mathbf{I}$. In the following Section 4 we provide the performance comparison for different WLS procedures.

4. Insights on the standard and optimal WLS position estimation

In this Section, we aim to compute the position covariance matrix for standard weighting matrices $\mathbf{W}$ and compare the results to assess the benefits of using the optimal weighting, exploiting not only delays ($\mathbf{W}_\tau = \beta\mathbf{P}_\alpha$) but also Dopplers ($\mathbf{W}_b = \delta\mathbf{P}_\alpha$). As the conventional processing only exploit the delays, we first consider the case of pseudoranges only multilateration.

4.1. Multilateration with pseudoranges only

In this case, $\mathbf{W}_b = \mathbf{0}$, so that $\boldsymbol{\Omega} = \mathbf{U}\mathbf{W}_\tau\mathbf{U}^T$, and (23) becomes

$$\mathrm{cov}(\mathbf{pos}) = c^2(\mathbf{U}\mathbf{W}_\tau\mathbf{U}^T)^{-1}(\mathbf{U}\mathbf{W}_\tau\mathbf{F}_\tau^{-1}\mathbf{W}_\tau\mathbf{U}^T)(\mathbf{U}\mathbf{W}_\tau\mathbf{U}^T)^{-1}. \tag{24}$$

As stated before, two procedures are conventionally used to compute the receiver position, namely the LS procedure, where $\mathbf{W}_\tau = \mathbf{I}$ and the WLS one, where the optimal weight is $\mathbf{W}_\tau = \beta\mathbf{P}_\alpha$. In the LS case, we have

$$\mathrm{cov}_{\mathrm{LS}}(\mathbf{pos}) = \frac{c^2}{\beta}(\mathbf{U}\mathbf{U}^T)^{-1}(\mathbf{U}\mathbf{P}_\alpha^{-1}\mathbf{U}^T)(\mathbf{U}\mathbf{U}^T)^{-1}. \tag{25}$$

In the WLS case, we have

$$\mathrm{cov}_{\mathrm{WLS}}(\mathbf{pos}) = \frac{c^2}{\beta}(\mathbf{U}\mathbf{P}_\alpha\mathbf{U}^T)^{-1}, \tag{26}$$

where we recall that $\mathbf{P}_\alpha = \mathrm{diag}(\boldsymbol{\alpha} \odot \boldsymbol{\alpha}^*)$ (i.e., $\mathbf{P}_\alpha(k,k) = |\alpha_k|^2$) is simply the matrix of the powers received on each satellite channel (conventionally measured by means of the carrier-to-noise density ratio C/N_0 in GNSS receivers). Hence, introducing a normalized direction vector manifold matrix $\mathcal{U}^T = \mathbf{P}_\alpha^{1/2}\mathbf{U}^T$, (26) reduces to

$$\mathrm{cov}_{\mathrm{WLS}}(\mathbf{pos}) = \frac{c^2}{\beta}(\mathcal{U}\mathcal{U}^T)^{-1}. \tag{27}$$

When computing the square root of the trace of this covariance matrix we recognize the so-called GDOP [1], through $(\mathrm{Tr}\{(\mathcal{U}\mathcal{U}^T)^{-1}\})^{1/2}$. In order to get rid of the unknown clock bias and focusing on the 3-D position parameters only, it is convenient to conduct a block inversion of $\mathcal{U}\mathcal{U}^T$. It is straightforward to obtain the covariance matrix on the position vector only, $\mathbf{p}$, as

$$\mathrm{cov}_{\mathrm{WLS}}(\mathbf{p}) = \frac{c^2}{\beta}(\mathcal{U}_c\mathcal{U}_c^T)^{-1} \tag{28}$$

where $\mathcal{U}_c = [(\mathbf{u}_{10} - -\mathbf{u}_0), \dots, (\mathbf{u}_{K0} - -\mathbf{u}_0)]\mathbf{P}_\alpha^{1/2}$, with $-\mathbf{u}_0 = \frac{\sum|\alpha_k|^2\mathbf{u}_{k0}}{\sum|\alpha_k|^2}$ the power-weighted mean direction vector. Hence, the position precision when using a WLS procedure is linked to the inverse of the covariance matrix driven by the weighted and centred unit vectors towards the visible satellites. In the special case where all the received signals have the same power, $\mathcal{U}_c\mathcal{U}_c^T$ is simply the covariance matrix of these unit vectors. This interpretation has already been noticed in [22], for instance.

4.2. Multilateration with both pseudoranges and dopplers

Now, we compute the position covariance matrix in the case where we use the complete information brought by the intermediate parameters (delays and Dopplers), with the aim to draw a comparison with the previous simplified, but widely used case. When using the optimal weighting matrices ($\mathbf{W}_\tau = \beta\mathbf{P}_\alpha, \mathbf{W}_b = \delta\mathbf{P}_\alpha$), the position covariance matrix (23) becomes,

$$\mathrm{cov}_{\mathrm{WLS}_{\mathrm{opt}}}(\mathbf{pos}) = c^2\left[\mathbf{U}\mathbf{F}_\tau\mathbf{U}^T + \mathbf{V}\mathbf{F}_b^{1/2}\mathbf{P}_\perp\mathbf{F}_b^{1/2}\mathbf{V}^T\right]^{-1}. \tag{29}$$

Again, introducing the power-normalized matrix $\mathcal{V}^T = \mathbf{P}_\alpha^{1/2}\mathbf{V}^T$, we can rewrite (29) as

$$\mathrm{cov}_{\mathrm{WLS}_{\mathrm{opt}}}(\mathbf{pos}) = c^2\left[\beta\mathcal{U}\mathcal{U}^T + \delta\mathcal{V}\mathbf{P}_\perp\mathcal{V}^T\right]^{-1}, \tag{30}$$

or

$$\mathrm{cov}_{\mathrm{WLS}_{\mathrm{opt}}}(\mathbf{pos}) = c^2\left[\beta\mathcal{U}\mathcal{U}^T + \delta\mathcal{V}_\perp\mathcal{V}_\perp^T\right]^{-1}, \tag{31}$$

where $\mathcal{V}_\perp^T = \mathbf{P}_\perp\mathcal{V}^T$. This last expression has to be compared with (27). We can see that this position covariance matrix, when using both delays and Dopplers, is composed of two terms. The first one is the same as in the delays only case, and is linked to the signal bandwidth, through β, and the GDOP, through $\mathcal{U}\mathcal{U}^T$. The second one, that will have a tendency to reduce the covariance matrix, is linked to the observation time, through δ and a kind of angular velocity GDOP, through $\mathcal{V}_\perp\mathcal{V}_\perp^T$. This last matrix is also similar to a covariance matrix driven by the angular velocity vectors contained in $\mathcal{V}$, after a projection onto the subspace orthogonal to $\mathcal{U}^T$. Hence, the more satellites we have, the smaller $\mathcal{V}_\perp\mathcal{V}_\perp^T$ is, as only the part

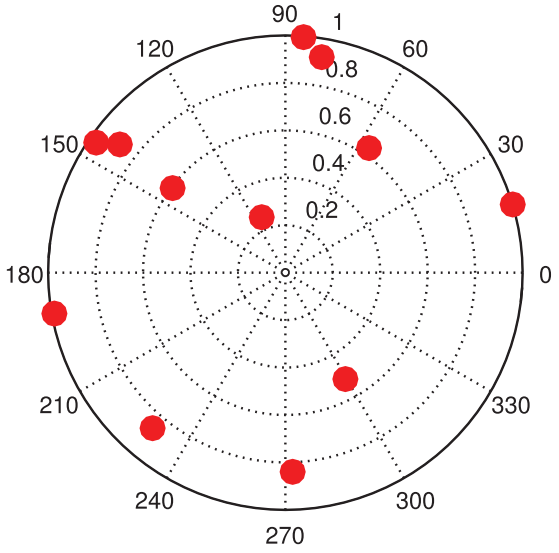

Fig. 1. Skyplot of the complete satellite configuration.

in the subspace orthogonal to the 4D subspace spanned by $\mathcal{U}^T$ remains. To go a step further, using the matrix inversion lemma, we have

$$\frac{1}{c^2}\text{cov}_{\text{WLS}_{\text{opt}}}(\mathbf{pos}) = \frac{(\mathcal{U}\mathcal{U}^T)^{-1}}{\beta} - \frac{(\mathcal{U}\mathcal{U}^T)^{-1}}{\beta}\mathcal{V}_\perp\left(\frac{\mathbf{I}}{\delta} + \mathcal{V}_\perp^T\frac{(\mathcal{U}\mathcal{U}^T)^{-1}}{\beta}\mathcal{V}_\perp\right)^{-1}\mathcal{V}_\perp^T\frac{(\mathcal{U}\mathcal{U}^T)^{-1}}{\beta}. \quad (32)$$

As noticed in [5], for a small integration time, $\mathcal{V}_\perp^T\frac{(\mathcal{U}\mathcal{U}^T)^{-1}}{\beta}\mathcal{V}_\perp$ is much smaller than $\frac{\mathbf{I}}{\delta}$ so that we can draw the following approximation

$$\frac{1}{c^2}\text{cov}_{WLS_{opt}}(\mathbf{pos}) \simeq \frac{(\mathcal{U}\mathcal{U}^T)^{-1}}{\beta} - \frac{(\mathcal{U}\mathcal{U}^T)^{-1}}{\beta}r(\mathcal{V}\mathbf{P}_\mathcal{U}^\perp\mathcal{V}^T)(\mathcal{U}\mathcal{U}^T)^{-1}, \quad (33)$$

where $r = \frac{\delta}{\beta} = \frac{f_0^2T_s^2(N-1)(N+1)}{B^2}$.

This approximation shows that the position covariance matrix, when using the appropriate delay and Doppler WLS scheme, is the one we obtained when using the delays only, but reduced by a correction matrix. This improvement correction matrix is inversely proportional to the covariance matrix on the direction vectors, $\mathcal{U}\mathcal{U}^T$, which shows that the improvement when including the Doppler information will be larger in case of bad geometries (i.e., bad GDOP). In other words, we can expect a better improvement in case of challenging environments, such as urban canyons, for instance.

5. Numerical simulations

To evaluate the gain provided by the optimal use of Doppler information, through the matched WLS procedure, we assess the positionig performance in 3 representative scenarios: (i) first, we consider an open-sky configuration with 12 satellites and a nominal $C/N_0 = 45$ dB-Hz; then, (ii) in order to discuss the impact of a constrained satellite visibility we limit the study to a constrained set of 6 satellites in a bad GDOP scenario; and finally, (iii) for completness we simulate a near indoor scenario with multipath and random signal attenuations.

5.1. Open-sky scenario

In this first simulation, we consider an ideal scenario where a GNSS receiver exploits GPS L1 C/A signals ($B = 1$ MHz) from 12 satellites. We consider the case where all the signals have the same nominal strength, $C/N_0 = 45$ dB-Hz. The satellite configuration is drawn from a real GPS constellation, through sp3 files, and the corresponding skyplot is presented in Fig. 1. The receiver has a constant speed of 15 m/s, for instance being the case of a car in an urban environment. Fig. 2 represents the square root of the trace of the position covariance matrices, limited to its first 3 elements, namely the position vector **p**. Adopting the standard GNSS nomenclature, this so-called Position Dilution Of Precision (PDOP) simply

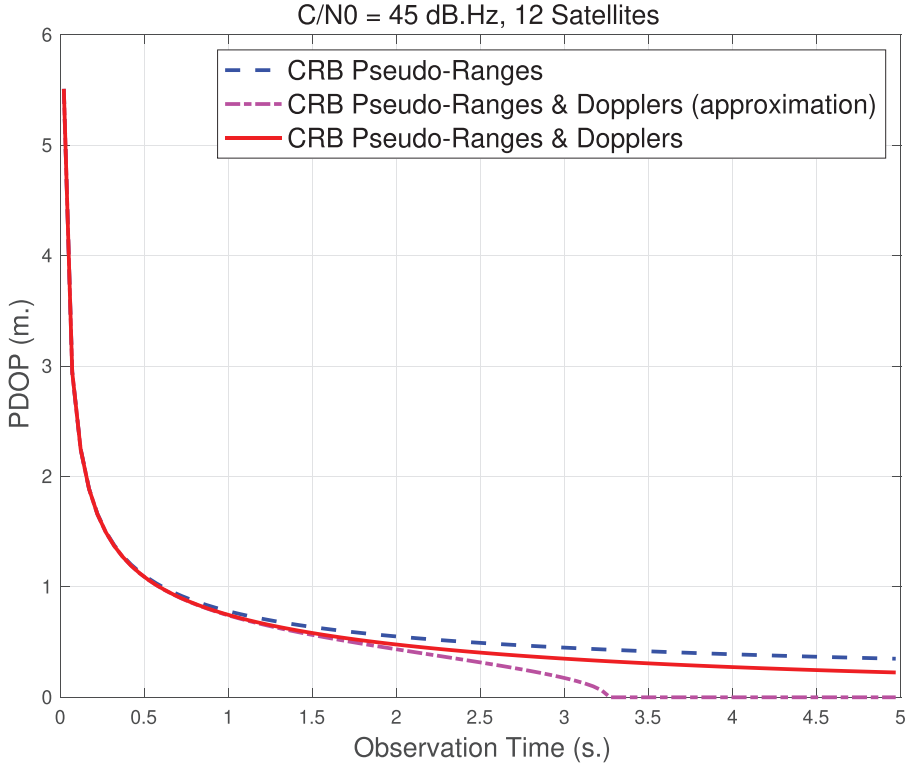

Fig. 2. Delay only vs. delay and Doppler CRB for position estimation (open-sky configuration). The CRB approximation is given in (33).

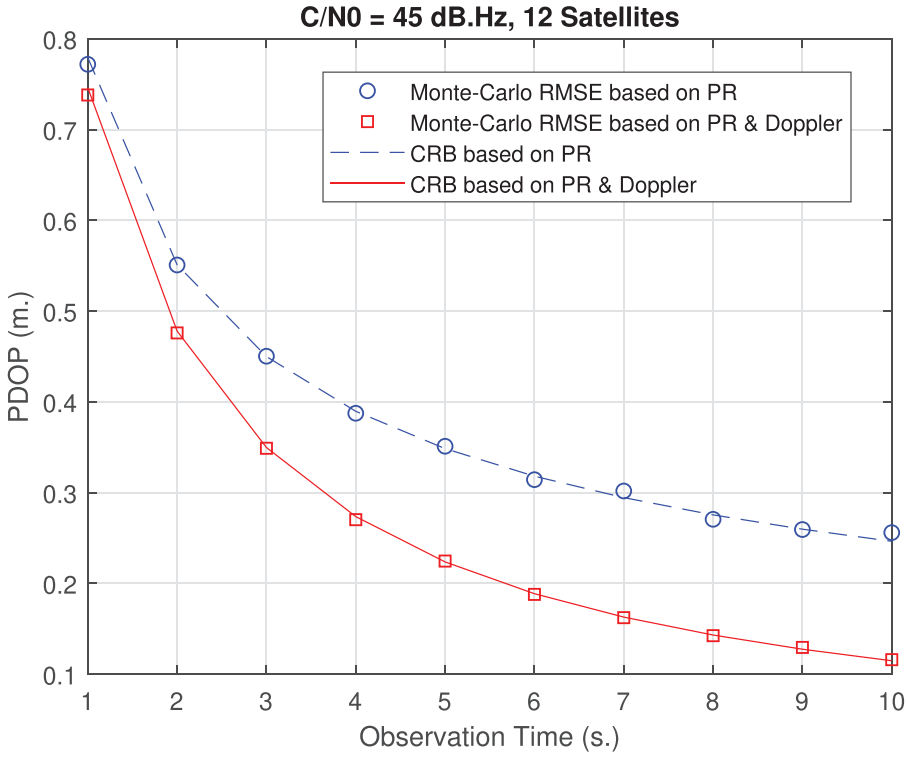

Fig. 3. Delay only vs. delay and Doppler RMSE and CRB for position estimation (open-sky configuration).

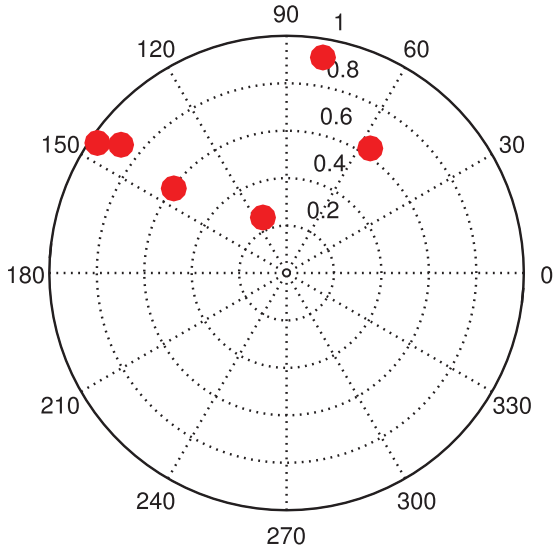

Fig. 4. Skyplot of a constrained satellite configuration.

represents the standard deviation of the position error, that is, the square-root of the trace of the CRB derived in this contribution. We compare the PDOP obtained with both (27), where the pseudoranges only are exploited, and (31), where pseudoranges and Dopplers are used. We have also plotted the approximation from (33). We can first notice that the proposed approximated formula is valid up to 2 s of integration time.

More interesting is the gain provided by the Doppler exploitation. In this open-sky configuration, the improvement seems weak, even if there is only a marginal additional computational cost in adding the Doppler information in the WLS procedure. For a short integration time in an open-sky scenario there is no apparent gain. But, although the majority of nowadays applications do not consider long integration times, there is a rising demand for improving the performance of GNSS systems in harsh environments. Indeed, under foliage canopy, urban canyons or indoor environment, conventional processing does not allow to recover the signals with C/N_0 up to 20 dB lower the nominal outdoor level. The main solution to compensate for these strong attenuations consists in increasing the integration time [19,23]. This so-called High Sensitivity GNSS (HS-GNSS) has attracted much attention during the last decade and some experiments tend to prove the practical benefits of such receivers for indoor pedestrian applications, for example [24]. But, while the main effort to improve the precision performance has been focused on the electronic sensitivity and the increase of the integration time, the second step of the processing usually remains the sub-optimal delay-based only WLS processing. This article proposes a complementary way of improvement in such long integration applications, using the Doppler information directly in the WLS position formulation. It also has to be noticed that in practical situations, the integration time is linked to the Frequency Lock Loop (FLL) filter bandwidth. In this case fractions of Hz of precision on the Doppler estimation can be achieved, corresponding to some seconds of integration time of this simulation.

To go a step further, and in order to assess the validity of the asymptotic covariance (CRB) derivation of this paper, we compare this results with estimated covariance errors obtained from Monte-Carlo simulations. To this end, Fig. 3 represents the same PDOP as Fig. 2, but with longer integration times, for both the asymptotic formulation given in this article and the estimated errors from 1000 Monte-Carlo simulations. First of all, we can observe a perfect match between the closed-form formulation of

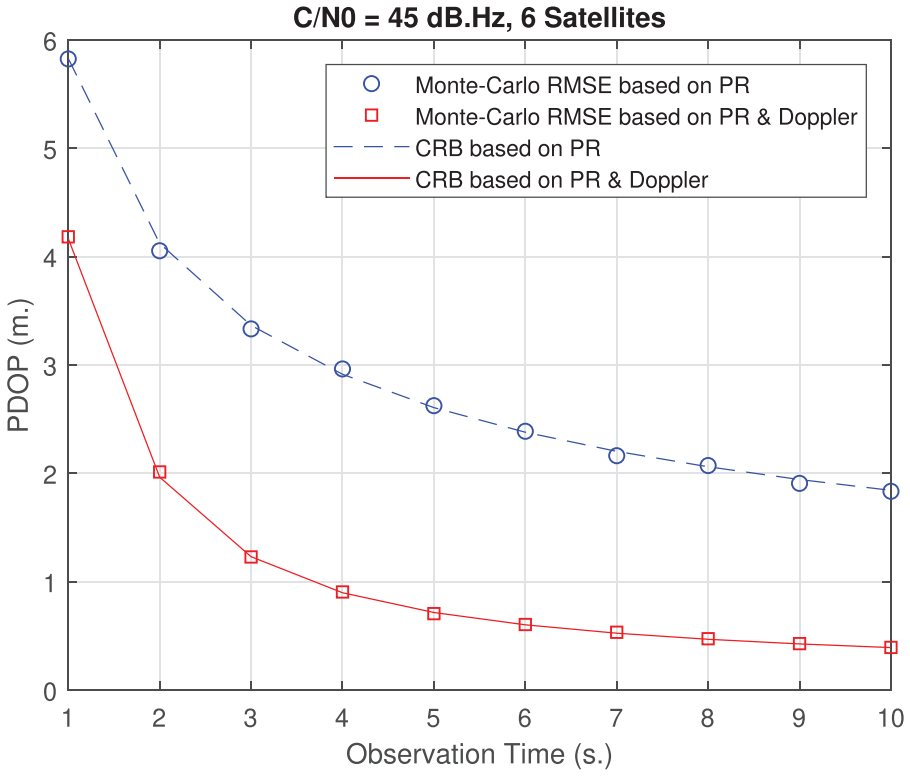

Fig. 5. Delay only vs. delay and Doppler RMSE and CRB for position estimation (constrained satellite visibility, i.e., urban canyon).

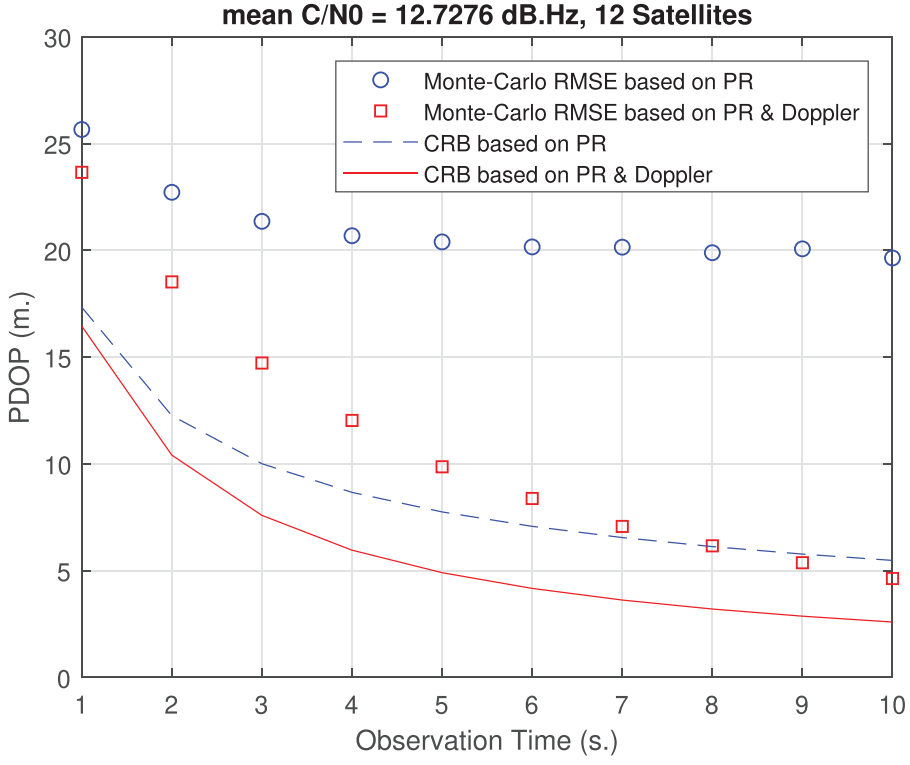

Fig. 6. Delay only vs. delay and Doppler RMSE and CRB for position estimation (near indoor (i.e, multipath and strong fadings) scenario).

this contribution and the Monte-Carlo results, which proves the validity of the present derivations. Moreover, in this open-sky scenario, the gain provided by Dopplers is about one third for integration times of 3 s, with almost no additional computing cost. It has to be noticed that when reaching such small precisions, other mismatches become the limiting error source to improve the positioning performance. But, the goal of this theoretical simulation is just to compare the precision brought by Dopplers with that of a delays-only solution, all other effects being removed. In addition, within this ideal situation, one could think on the use of Doppler information within PPP approaches, where the majority of defaults have been removed and where we need long observation time to converge to a precise solution.

5.2. Constrained satellite visibility (Bad GDOP) scenario

As it can be noticed when analysing the approximated expression (33), we can expect a higher gain in bad GDOP scenarios. To this end, we consider the case with only a subset of 6 out of the 12 visible satellites, all belonging to a restricted section of the sky, as represented on the skyplot in Fig. 4. This satellite visibility configuration is representative of a standard urban environment, where some directions are blocked by buildings. Again, notice that the use of a realistic urban canyon propagation channel is out of the scope of this contribution, but considering a bad/constrained satellite geometry illustrates the possible benefits in such conditions. As expected, a larger improvement due to the Doppler usage in this more degraded GDOP scenario is shown in Fig. 5. In this case the precision is twice better, when Dopplers are used, with 2 s of integration time. As in the previous case, the RMSE obtained through Monte-Carlo simulations matches the corresponding theoretical CRB.

5.3. Near indoor (multipath and strong fadings) scenario

To complete the discussion, we assess the CRB and RMSE positioning performance for a near indoor scenario where the receiver is assumed to be at a fixed position. In this case, we consider again the 12 satellites as in the open-sky scenario, but with: (i) a random multipath, uniformly distributed over $[0-100]$ m, and (ii) strong signal attenuations, conducting to signal strengths uniformly distributed over $[0-20]$ dB-Hz. Notice that the CRB derived in this contribution does not consider multipath propagation conditions, a result which is not even available in the literature for the delay-only case, therefore, as it was the case in the previous scenarios the RMSE is not expected to match such CRB.

The PDOP when using the Doppler information or not, both for the asymptotic formulation derived in this paper and the Monte-Carlo simulations, is shown in Fig. 6. First, as already stated, the closed-form formulation does not match the Monte-Carlo results, as the multipath degrades the performances. Second, it is remarkable that the improvement when using Dopplers is larger in the multipath case (i.e, Monte-Carlo simulations) than in the nominal one (i.e, CRB). This is due to the lower sensitivity of Dopplers to multipath with respect to code-based pseudoranges. These results further support and complement the discussion in the two previous scenarios: (i) under nominal conditions Dopplers bring a benefit for integration times $>$ 1 s, (ii) this improvement is larger for constrained satellite visibility or bad GDOPs as expected from (31) and (33), and (iii) because Dopplers are less sensitive to multipath, the performance gain is even more evident under harsh propagation conditions.

6. Conclusions

In this paper, we addressed the problem of evaluating the performance of positioning in the GNSS context. The position estimation is both related to the delays and Dopplers, although this last piece of information is conventionally not properly used in GNSS receivers. We provided a closed-from and simple formulation of the position precision through the corresponding CRB, that allows to analyse the gain associated to the optimal use of Doppler information. This precision formulation is valid for any kind of WLS procedure, including the standard case based on the delays only. We showed that the improvement using Dopplers could be significant in situations where a long observation time is needed, such as HS-GNSS applications (i.e., indoor conditions or space exploration). The gain brought by Doppler information is larger in challenging conditions with a constrained satellite constellation geometry (poor GDOP), as in urban canyons. Moreover, in these harsh propagation conditions an additional disturbance is multipath. It was showed that because Dopplers are less sensitive to multipath than code-based measurements, the improvement brought by Dopplers is even larger. Finally, exploiting Dopplers could also be a solution of choice for reducing the convergence time of PPP algorithms.

Declaration of Competing Interest

The authors declare that they have no known competing financial interests or personal relationships that could have appeared to influence the work reported in this paper.

Appendix A. Intermediate Parameters FIM

We first recall some useful results for GNSS signals. Some of these results have been proven in [5] and are completed here. As shown in [5], we know that

$$R_{k,l}(\tau_l-\tau_k)=\int c_k(t-\tau_k)c_l(t-\tau_l)e^{-2i\pi f_0(b_k-b_l)t}dt\simeq 0, \qquad \forall \tau_l,\tau_k,b_l,b_k \quad if\ k\neq l. \tag{A.1}$$

Hence,

$$\frac{\partial^2 R_{k,l}(\tau_l-\tau_k)}{\partial\tau_l\partial\tau_k}=\int \cdot c_k(t-\tau_k)\cdot c_l(t-\tau_l)e^{-2i\pi f_0(b_k-b_l)t}dt\simeq 0, \qquad \forall \tau_l,\tau_k,b_l,b_k \quad if\ k\neq l. \tag{A.2}$$

Moreover, if we write $\cdot\mathbf{c_k}=[\cdot c_k(-\tau_k),\cdots,\cdot c_k((N-1)T_s-\tau_k)]^T$, we know, from [5] that

$$\cdot\mathbf{c_k}^T\cdot\mathbf{c_k}=\frac{\pi^2B^2N}{3}. \tag{A.3}$$

Gathering (A.2) and (A.3), we can write

$$(\cdot\mathbf{c_k}\odot\mathbf{e_k})^H(\cdot\mathbf{c_l}\odot\mathbf{e_l})=\delta(k-l)\frac{\pi^2B^2N}{3}.$$

Furthermore, letting $\tau_l=0$ in (A.1) we have

$$\int c_k(t-\tau_k)c_l(t)e^{-2i\pi(f_k-f_l)t}dt\simeq 0,\ \text{if } k\neq l.$$

Using Parceval's identity we can write

$$\int C_k(f+f_k)e^{-2i\pi(f+f_k)\tau_k}C_l^*(f+f_l)df\simeq 0,\ \text{if } k\neq l,$$

where $C_k(f)$ is the Fourier transform of $c_k(t)$. Hence, differentiating with respect to f_l we have

$$0 \simeq \int C_k(f+f_k)e^{-2i\pi(f+f_k)\tau_k}\frac{\partial C_l(f+f_l)}{\partial f_l}df$$
$$= \int (2i\pi t)c_k(t-\tau_k)c_l(t)e^{-2i\pi(f_k-f_l)t}dt.$$

Now, differentiating with respect to τ_k, we can deduce that

$$\int t{\cdot}c_k(t-\tau_k)c_l(t)e^{-2i\pi(f_k-f_l)t}dt \simeq 0, \text{ if } k \neq l. \tag{A.4}$$

Moreover,

$$\int t{\cdot}c_k(t-\tau_k)c_k(t-\tau_k)dt \tag{A.5}$$
$$= \left[tc_k^2(t-\tau_k)\right] - \int c_k(t-\tau_k)(c_k(t-\tau_k)+t{\cdot}c_k(t-\tau_k))dt$$
$$= [t] - \int c_k^2(t-\tau_k)dt - \int tc_k(t-\tau_k){\cdot}c_k(t-\tau_k))dt$$
$$= -\int tc_k(t-\tau_k){\cdot}c_k(t-\tau_k))dt,$$

so that

$$\int t{\cdot}c_k(t-\tau_k)c_k(t-\tau_k)dt = 0. \tag{A.6}$$

Gathering (A.4) and (A.6), we can conclude that

$$(\mathbf{t}\odot{\cdot}\mathbf{c_k}\odot\mathbf{e_k})^H(\mathbf{c_l}\odot\mathbf{e_l}) \simeq 0, \ \forall\, k,l$$

where $\mathbf{t} = T_s[0\cdots(N-1)]^T$.

To sum-up all these intermediate results,

$$(\mathbf{t}\odot\mathbf{t}\odot\mathbf{c_k}\odot\mathbf{e_k})^H(\mathbf{c_l}\odot\mathbf{e_l}) = \delta(k-l)\,T_s^2\sum_{n=0}^{N-1}n^2,$$

$$\mathbf{a}_k^H(\cdot\mathbf{c}_l\odot\mathbf{e}_l) = 0, \quad \forall\, k,l$$

$$\mathbf{a}_k^H(\mathbf{t}\odot\mathbf{a}_l) = \delta(k-l)T_s\sum_{n=0}^{N-1}n,$$

$$(\mathbf{t}\odot{\cdot}\mathbf{c_k}\odot\mathbf{e_k})^H(\mathbf{c_l}\odot\mathbf{e_l}) \simeq 0, \ \forall\, k,l$$

$$({\cdot}\mathbf{c_k}\odot\mathbf{e_k})^H({\cdot}\mathbf{c_l}\odot\mathbf{e_l}) = \delta(k-l)\frac{\pi^2B^2N}{3},$$

where $\mathbf{t} = T_s[0\cdots(N-1)]^T$ and ${\cdot}\mathbf{c_k} = [{\cdot}c_k(-\tau_k),\cdots,{\cdot}c_k((N-1)T_s-\tau_k)]^T$.

Now, considering (19), we have to compute the first derivatives with respect to the unknown intermediate parameters,

$$\frac{\partial\mathbf{A}\boldsymbol{\alpha}}{\partial\mathrm{Re}\{\alpha_k\}} = \mathbf{a}_k,$$
$$\frac{\partial\mathbf{A}\boldsymbol{\alpha}}{\partial\mathrm{Im}\{\alpha_k\}} = i\mathbf{a}_k,$$
$$\frac{\partial\mathbf{A}\boldsymbol{\alpha}}{\partial\tau_k} = -\alpha_k{\cdot}\mathbf{c}_k\odot\mathbf{e}_k,$$
$$\frac{\partial\mathbf{A}\boldsymbol{\alpha}}{\partial b_k} = (-2i\pi f_0\alpha_k)\,\mathbf{t}\odot\mathbf{a}_k.$$

Using the preliminary results above, it is straightforward to compute the FIM over $\boldsymbol{\gamma}$,

$$\mathbf{F}_{\boldsymbol{\gamma}}(\mathrm{Re}\{\alpha_k\},\mathrm{Re}\{\alpha_\ell\}) = \frac{2}{\sigma^2}\mathrm{Re}\left\{\mathbf{a}_k^H\mathbf{a}_\ell\right\} \simeq \frac{2N}{\sigma^2}\delta(k-\ell),$$

$$\mathbf{F}_{\boldsymbol{\gamma}}(\mathrm{Re}\{\alpha_k\},\mathrm{Im}\{\alpha_\ell\}) = \frac{2}{\sigma^2}\mathrm{Re}\left\{i\mathbf{a}_k^H\mathbf{a}_\ell\right\} = 0,$$

$$\mathbf{F}_{\boldsymbol{\gamma}}(\mathrm{Im}\{\alpha_k\},\mathrm{Im}\{\alpha_\ell\}) = \frac{2}{\sigma^2}\mathrm{Re}\left\{(i\mathbf{a}_k)^Hi\mathbf{a}_\ell\right\} \simeq \frac{2N}{\sigma^2}\delta(k-\ell),$$

$$\mathbf{F}_{\boldsymbol{\gamma}}(\mathrm{Re}\{\alpha_k\},\tau_\ell) = \frac{2}{\sigma^2}\mathrm{Re}\left\{-\alpha_\ell\mathbf{a}_k^H(\cdot\mathbf{c}_\ell\odot\mathbf{e}_\ell)\right\} = 0,$$

$$\mathbf{F}_{\boldsymbol{\gamma}}(\mathrm{Im}\{\alpha_k\},\tau_\ell) = \frac{2}{\sigma^2}\mathrm{Re}\left\{i\alpha_\ell\mathbf{a}_k^H(\cdot\mathbf{c}_\ell\odot\mathbf{e}_\ell)\right\} = 0,$$

$$\mathbf{F}_{\boldsymbol{\gamma}}(\mathrm{Re}\{\alpha_k\},b_\ell) = \frac{2}{\sigma^2}\mathrm{Re}\left\{(-2i\pi f_0\alpha_\ell)\,\mathbf{a}_k^H(\mathbf{t}\odot\mathbf{a}_\ell)\right\}$$
$$= \delta(k-\ell)\,\frac{4\pi f_0\mathrm{Im}\{\alpha_k\}}{\sigma^2}T_s\sum_{n=0}^{N-1}n,$$

$$\mathbf{F}_{\boldsymbol{\gamma}}(\mathrm{Im}\{\alpha_k\},b_\ell) = \frac{2}{\sigma^2}\mathrm{Re}\left\{(-2\pi f_0\alpha_\ell)\,\mathbf{a}_k^H(\mathbf{t}\odot\mathbf{a}_\ell)\right\}$$
$$= -\delta(k-\ell)\,\frac{4\pi f_0\mathrm{Re}\{\alpha_k\}}{\sigma^2}T_s\sum_{n=0}^{N-1}n,$$

$$\mathbf{F}_{\boldsymbol{\gamma}}(\tau_k,\tau_\ell) = \frac{2}{\sigma^2}\mathrm{Re}\left\{(\alpha_k{\cdot}\mathbf{c}_k\odot\mathbf{e}_k)^H(\alpha_\ell{\cdot}\mathbf{c}_\ell\odot\mathbf{e}_\ell)\right\}$$
$$= \delta(k-\ell)|\alpha_k|^2\frac{2\pi^2B^2}{3\sigma^2}\frac{N}{},$$

$$\mathbf{F}_{\boldsymbol{\gamma}}(\tau_k,b_\ell) = \frac{2}{\sigma^2}\mathrm{Re}\left\{(\alpha_k{\cdot}\mathbf{c}_k\odot\mathbf{e}_k)^H((2i\pi f_0\alpha_\ell)\,\mathbf{t}\odot\mathbf{a}_\ell)\right\} = 0,$$

$$\mathbf{F}_{\boldsymbol{\gamma}}(b_k,b_\ell) = \frac{2}{\sigma^2}\mathrm{Re}\left\{((2i\pi f_0\alpha_k)\,\mathbf{t}\odot\mathbf{a}_k)^H((2i\pi f_0\alpha_\ell)\,\mathbf{t}\odot\mathbf{a}_\ell)\right\}$$
$$= \delta(k-\ell)|\alpha_k|^2\frac{8\pi^2f_0^2T_s^2\sum_{n=0}^{n-1}n^2}{\sigma^2}.$$

References

[1] E.D. Kaplan, C.J. Hegarty, Understanding GPS. Principles and Applications, Artech House Publishers, 1996.
[2] A. Dogandzic, A. Nehorai, Cramér-Rao bounds for estimating range, velocity, and direction with an active array, IEEE Trans. Signal Process. 49 (6) (2001) 1122–1137.
[3] Y. Chen, R.S. Blum, On the impact of unknown signals on delay, doppler, amplitude, and phase parameter estimation, IEEE Trans. Signal Process. 67 (2) (2019) 431–443.
[4] P.J.G. Teunissen, O. Montenbruck (Eds.), Handbook of Global Navigation Satellite Systems, Springer, Switzerland, 2017.
[5] F. Vincent, E. Chaumette, C. Charbonnieras, J. Israel, L. Ries, M. Aubourg, F. Barbiero, Asymptotically efficient GNSS trilateration, Signal Process., 133 (2017) 270–277.
[6] P. Closas, C. Fernández-Prades, J.A. Fernández-Rubio, Maximum likelihood estimation of position in GNSS, IEEE Signal Process. Lett., 14 (2007) 359–362.
[7] P. Closas, A. Gusi-Amigó, Direct position estimation of GNSS receivers, IEEE Signal Process. Mag. 34 (5) (2017) 72–84.
[8] S. Choy, S. Bisnath, C. Rizos, Uncovering common misconceptions in GNSS precise point positioning and its future prospect, GPS Solut. 21 (2017) (2017).
[9] N. Othieno, S. Gleason, Combined Doppler and time free positioning technique for low dynamics receivers, in: Proceedings of the IEEE/ION Position, Location and Navigation Symposium, 2012.
[10] D. Medina, J. Vilà-Valls, E. Chaumette, F. Vincent, P. Closas, Cramér-Rao bound for a mixture of real- and integer-valued parameter vectors and its application to the linear regression model, Signal Process. (2020).
[11] P. Closas, C. Fernández-Prades, J.A. Fernández-Rubio, Cramér-Rao bound analysis of positioning approaches in GNSS receivers, Signal Process. 57 (10) (2009) 3775–3786.
[12] P. Stoica, T. Soderstrom, On reparametrization of loss functions used in estimation and the invariance principle, Signal Process. 17 (4) (1989) 383–387.
[13] A. Amar, A.J. Weiss, Localization of narrowband radio emitters based on doppler frequency shifts, Signal Process. 56 (11) (2008) 5500–5508.
[14] A.J. Weiss, A. Amar, Direct position determination of multiple radio signals, EURASIP J. Appl. Signal Process. (2005) 37–49.
[15] A.J. Weiss, Direct geolocation of wideband emitters based on delay and doppler, IEEE Trans. Signal Process. 59 (6) (2011) 2513–2521.
[16] J.G. Erling, M.J. Roan, M.R. Gramann, Performance bounds for multisource parameter estimation using a multiarray network, IEEE Trans. Signal Process. 55 (10) (2007) 4791–4799.
[17] R.J. Kozick, B.M. Sadler, Source localization with distributed sensor array and partial spatial coherence, IEEE Trans. Signal Process. 52 (3) (2004) 1–17.

[18] D. Pascual, A. Camps, F. Martin, H. Park, A.A. Arroyo, R. Onrubia, Precision bounds in GNSS-R ocean altimetry, IEEE J. Sel. Top. Appl. Earth Observ. Remote Sens. 7 (5) (2014) 1416–1422.
[19] G. Seco-Granados, J.A. Lopez-Salcedo, D. Jiménez-Banos, G. López-Risueno, Challenges in indoor global navigation satellite systems. unveiling its core features in signal processing, IEEE Signal Process. Mag. 29 (2) (2012) 108–131.
[20] S. Bancroft, An algebraic solution of the GPS equations, IEEE Trans. Aerosp. Electron. Syst. 21 (1985) 56–69.
[21] P. Groves (Ed.), Principles of GNSS, Inertial, and Multisensor Integrated Navigation Systems, Artech House, United Kingdom, 2013.
[22] J. Chaffee, J. Abel, GDOP and the CramÉr-Rao Bound, in: Proceedings of IEEE Position, Location and Navigation Symposium - PLANS'94, Las Vegas, NV, 1994.
[23] Z. He, V. Renaudin, M.G. Petovello, G. Lachapelle, Use of high sensitivity GNSS receiver doppler measurements for indoor pedestrian dead reckoning, Sensors 13 (2013) 4303–4326.
[24] G.A. Vecchione, DINGPOS, a GNSS-Based Multi-sensor Demonstrator for Indoor Navigation: Preliminary Results, Position Location and Navigation Symposium (PLANS), IEEE/ION, Indian Wells, CA, USA, 2010.